UNCLASSIFIED

SECURITY CLASSIFICATION OF THIS PAGE (When Data Entered)

DTIC FILE COPY

1

REPORT DOCUMENTATION PAGE		READ INSTRUCTIONS BEFORE COMPLETING FORM
1. REPORT NUMBER AFIT/CI/NR 88- 156	2. GOVT ACCESSION NO.	3. RECIPIENT'S CATALOG NUMBER
4. TITLE (and Subtitle) CONCENTRATION GRADIENT DETECTION BY NEAR-INFRARED DIODE LASER INTERFEROMETRY		5. TYPE OF REPORT & PERIOD COVERED MS THESIS 6. PERFORMING ORG. REPORT NUMBER
7. AUTHOR(s) DARRELL O. HANCOCK		8. CONTRACT OR GRANT NUMBER(s)
9. PERFORMING ORGANIZATION NAME AND ADDRESS AFIT STUDENT AT: UNIVERSITY OF WASHINGTON		10. PROGRAM ELEMENT, PROJECT, TASK AREA & WORK UNIT NUMBERS
CONTROLLING OFFICE NAME AND ADDRESS		12. REPORT DATE 1988 13. NUMBER OF PAGES 53
MONITORING AGENCY NAME & ADDRESS (if different from Controlling Office) AFIT/NR Wright-Patterson AFB OH 45433-6583		15. SECURITY CLASS. (of this report) UNCLASSIFIED 15a. DECLASSIFICATION DOWNGRADING SCHEDULE

AD-A196 197

16. DISTRIBUTION STATEMENT (of this Report)

DISTRIBUTED UNLIMITED: APPROVED FOR PUBLIC RELEASE

DTIC ELECTE AUG 04 1988 S D

17. DISTRIBUTION STATEMENT (of the abstract entered in Block 20, if different from Report)

SAME AS REPORT

18. SUPPLEMENTARY NOTES

Approved for Public Release: IAW AFR 190-1
LYNN E. WOLAVER 21 July 88
Dean for Research and Professional Development
Air Force Institute of Technology
Wright-Patterson AFB OH 45433-6583

19. KEY WORDS (Continue on reverse side if necessary and identify by block number)

20. ABSTRACT (Continue on reverse side if necessary and identify by block number)

ATTACHED

DD FORM 1 JAN 73 1473 EDITION OF 1 NOV 65 IS OBSOLETE

UNCLASSIFIED

SECURITY CLASSIFICATION OF THIS PAGE (When Data Entered)

ABSTRACT

CONCENTRATION GRADIENT DETECTION BY
NEAR-INFRARED DIODE LASER INTERFEROMETRY.
Darrell O. Hancock, Capt, USAF. 1988, 53 pgs., MS,
University of Washington.

Concentration gradient detection is performed with a diode laser system which probes the associated refractive index gradient (RIG). The detector has excellent potential for both High Performance Liquid Chromatography (HPLC) and Flow Injection Analysis (FIA). The RIG detector measured 280 picograms (3 x rms) of injected polystyrene following size-exclusion chromatography (SEC). A version incorporating a position sensitive detector in lieu of interferomatic measurement allows laser beam deflection angles of less than 2.4 microradians to be measured. The system performance as a universal detector for HPLC is contrasted with UV-Vis detection. The device is clearly superior to UV-Vis detection of species that are not highly absorbing. RIG sensitivity to solute peak broadening also promises rapid polymer characterization potential with a FIA scheme.

Key Sources: Hancock, D.O.; Synovec, R.E. Anal. Chem. 1988, (submitted).

Renn, C.N.; Synovec, R.E. Anal. Chem. 1988, 60,200-204.

Born, M.; Wolf, E. Principles of Optics, 6th ed., 1980, Pergamon Press, Great Britain, pp.121-1240.

Yeung, E.S.; Synovec, R.E. Anal. Chem. 1986, 58, 1237A-1256A.

Pawliszyn, J. Anal. Chem. 1986, 58, 243-246.

Pawliszyn, J. Anal. Chem. 1986, 58, 3207-3215.

Concentration Gradient Detection by Near-Infrared

Diode Laser Interferometry

by

DARRELL O. HANCOCK

A thesis submitted in partial fulfillment
of the requirements for the degree of

Master of Science

University of Washington

1988

Approved by Robert E Synovec
(Chairperson of Supervisory Committee)

Program Authorized
to Offer Degree CHEMISTRY

Date May 23, 1988

Master's Thesis

In presenting this thesis in partial fulfillment of the requirements for a Master's degree at the University of Washington, I agree that the Library shall make its copies freely available for inspection. I further agree that extensive copying of this thesis is allowable only for scholarly purposes, consistent with "fair use" as prescribed in the U.S. Copyright Law. Any other reproduction for any purposes or by any means shall not be allowed without my written permission.

Signature_____

Date_____

TABLE OF CONTENTS

LIST OF FIGURES

LIST OF TABLES

ACKNOWLEDGMENTS

The author expresses sincere appreciation for the help and guidance by Assistant Professor Robert E. Synovec in all aspects of the research resulting in this manuscript. Thanks is also given to Professor Gary D. Christian and Lloyd Burgess for their many suggestions and helpful comments. Professor Callis and the Center for Process Analytical Chemistry are thanked for their support of this work. Thanks also to my good friend, Curtiss Renn, who always gave more than could possibly be repaid.

DEDICATION

This work is dedicated to my wife, Rebecca, who may not understand what is written herein, but has always understood what is inside of me.

Introduction

Since the advent of lasers in the early 1960's, considerable research has been conducted toward their use in a vast variety of analytical instrumentation. The extraordinary properties of laser light (compared to other light sources) - namely high power, ease in focusing, high coherence, monochromaticity and high degree of polarization purity (1) have all been capitalized upon in instrumental design. Analytical chemistry instrumentation often features the laser as a probe beam. That is, a cell containing chemical species is probed by the laser beam and, information about changes occurring in the chemical system within the cell are encoded in the beam from which pertinent chemical and physical information is extracted after beam detection. The trend has generally been toward higher power lasers and better monochromaticity, which is in accord with the analytical chemist's quest for increased sensitivity and better selectivity.

Semiconductor diode lasers have unique advantages as probe beams compared to their high energy counterparts, advantages which are only recently being exploited in analytical chemistry instrumentation. Diode lasers are the least expensive and smallest lasers available (1) and are much more rugged and efficient than the larger lasers. These reasons alone make the diode laser appealing for use in instrumentation, but the large angular spread of the characteristic diode laser fan beam presents a drawback for

some applications, and current wavelength limitations to a few near-infrared bands have especially deterred spectroscopists. Only recently have diode lasers which operate in the visible spectrum been reported (2). However, few chemical species absorb strongly at typical diode laser frequencies (750 nm - 1550 nm), which is a distinct advantage for some optical techniques based upon refractive index changes. The diode laser also is extremely stable with essentially no mode-hopping and coherence lengths of up to 40 meters. Such stability and coherence make the diode laser extremely attractive in many applications. No elaborate power supply is required and often thermostatting is generally not required, although thermoelectric cooling does enhance the diode laser efficiency and power stability (1).

In this work, the unique characteristics of the diode laser have been exploited to construct a novel system which provides for detection of concentration gradients by responding to associated refractive index gradients. The detector is demonstrated as an HPLC detector and as a detector for simple flowing systems.

Recently, HPLC detector development has had vigorous activity (3-6), with detectors designed with a variety of important characteristics, i.e., sensitivity, selectivity or universality, robustness, and overall solute identification or characterization capability. Often, selectivity and

sensitivity in HPLC detection are positively correlated, such as with absorbance or fluorescence detection, which leads to favorable detection limits and better detector applicability to samples of interest. Within this context, universal detection is quite popular since analyte derivatization is not required, while more sensitive methods, such as fluorescence, often require analyte derivatization. Unfortunately universal detectors, such as a refractive index (RI) detector, generally have limited applicability when dilute samples are encountered, due to limited sensitivity.

Ideally, a highly sensitive universal detector should be developed that does not require sample derivatization to enhance sensitivity. With universal detection, it is often difficult to utilize gradient elution, since the solvent contributes strongly to the baseline signal. The ideal universal detector would be highly resilient to solvent gradients. Thus, as Stolyhwo, Colin and Guichon pointed out (7), analogous to the flame ionization detector (FID) in gas chromatography, a sensitive universal detector for HPLC is not available. They developed a light scattering (LS) detector for HPLC based upon an evaporative nebulization process (7,8). The evaporative LS has many favorable properties, yet unfortunately requires evaporation of the eluting solvent-solute mixture with preferential evaporation of the solvent. Further, the LS detector has moderate

sensitivity compared to RI or absorbance detection (7). These factors may limit the overall universality of this LS detector, although excellent separations based upon gradients are feasible (8). A second approach to obtain "universal" detection in HPLC involves absorbance detection in the UV range of 185-210 nm (9-11). Selected solvents were investigated to assess their transparency in this UV range. The list of solvents available as eluents for "universal" absorbance detection at 185-210 nm was quite useful, yet may be limiting in many instances. A third approach to universal detection involves indirect solute detection (12-14). A property of the solvent is exclusively monitored by the detector thus producing a "high" background signal. Displacement of the solvent (eluent) by a solute results in a net reduction in the solvent concentration as the solute/solvent mixture passes through the detector. This produces a negative detector response, i.e., an indirect solute signal. While indirect detection provides easy solute quantitation, solute characterization would require a second form of detection, i.e., another detector sensitive to some physical property of the solute(s) of interest.

One realizes that RI dection remains the workhorse of everyday universal HPLC detectors. RI is a well understood chemical property, that has led to new approaches to chemical analysis, i.e., complex sample characterization

without analyte standards (15-18). RI detectors have been developed based upon four basic designs: refraction, reflection, interference, and the Christiansen effect (4). State-of-the-art, in terms of RI detectability and detector robustness, varies for these designs. For capillary and microbore HPLC, Bornhop and Dovichi suggested an interesting refraction-type RI detector based upon a capillary flow cell (19). They applied the novel device in the reversed phase microbore separation and RI detection of nanogram quantities of sugars (20). Further, they combined the capillary flow cell based RI detector with simultaneous absorbance detection (21). When optimized, this capillary flow cell based RI detector appears to be limited to about 3 x 10^{-7} RI units (3 x rms) as the limit-of-detection (LOD) when optimized (22). This detector is highly robust and simple to produce and maintain. The second type of RI detector, reflection-based, was optimized by Wilson and Yeung (23). They achieved a RI signal based upon the change in transmitted light at a liquid-glass interface, in accordance with Snell's and Fresnel's laws. Their device allowed for simultaneous RI, absorbance, and fluorescence detection with a 1 cm pathlength through the cell, in only about 1 uL volume. RI detectability was comparable to the capillary based RI detector (refraction-based), at about 1 x 10^{-7} RI units. The interference-type RI detector (24) yields an excellent LOD at 4 x 10^{-9} RI units, yet, a relatively long

pathlength, in the context of microbore or capillary HPLC, was required. The Christiansen effect RI detector has had few developments recently (4). Gradient applications with RI detection have been limited, since most consider this impractical if not impossible, yet gradients may be applied with RI detection by employing a volume delay loop for dual-cell RI detectors (25). Ideally, one would desire to utilize gradients in RI detection without requiring a volume delay loop which contributes to solute peak broadening.

Recently, Pawliszyn proposed an interesting approach to RI detection, based upon probing the RI gradient (26). The nature of the detected signal was attributed to a Schlieren effect. The sheath flow technique was applied to enhance detector sensitivity. In subsequent studies of the detector properties (27), it was determined that the sensitivity was pathlength dependent, thus scaling down the device may sacrifice sensitivity. A predicted detection limit of 3×10^{-8} RI units LOD was reported (27). A very interesting consequence of measuring the refractive index gradient (RIG) was realized, i.e., for linear eluent gradients, the RIG detector yields a rather small, constant, baseline offset (27). Thus, the RIG detector readily allows for use of eluent gradients, while providing excellent solute detectabilities. In this initial work on RIG detection (26,27) the nature of the detected signal was not fully described, and approaches for improving the device were not

addressed. Since interferometry is the most sensitive RI detection method available (24), one may expect to improve RIG detection similarly by an interferometric design.

This research involved constructing and studying a sensitive RIG interferometric sensor. The device employs common path interferometry to provide a sensitive measure of probe beam deflection (28-30). Thus, a simple interferometric sensor has been developed that measures RIG effects. The complete system is shown in Figure 1. The diode laser, flow cell, flow cell windows and photodiode are the components that comprise the interferometric sensor. Measurement of femtomole quantities of injected polymers, separated by microbore size-exclusion HPLC, with RIG detection was demonstrated, corresponding to 4 x 10^{-9} units (3 x rms) detectability. This was accomplished at a non-absorbing wavelength for the eluent and the polymers (780 nm). The novel device was relatively simple to construct and employ, although the shape of the observed solute response is atypical of conventional HPLC detectors, since the solute concentration gradient is monitored, instead of the solute concentration. The new detector has many attributes that may lead one to believe that the ideal universal detector for HPLC is forthcoming. The detection principle of gradient detection is outlined, prior to discussing salient experimental parameters, system optimization, and subsequent detector performance.

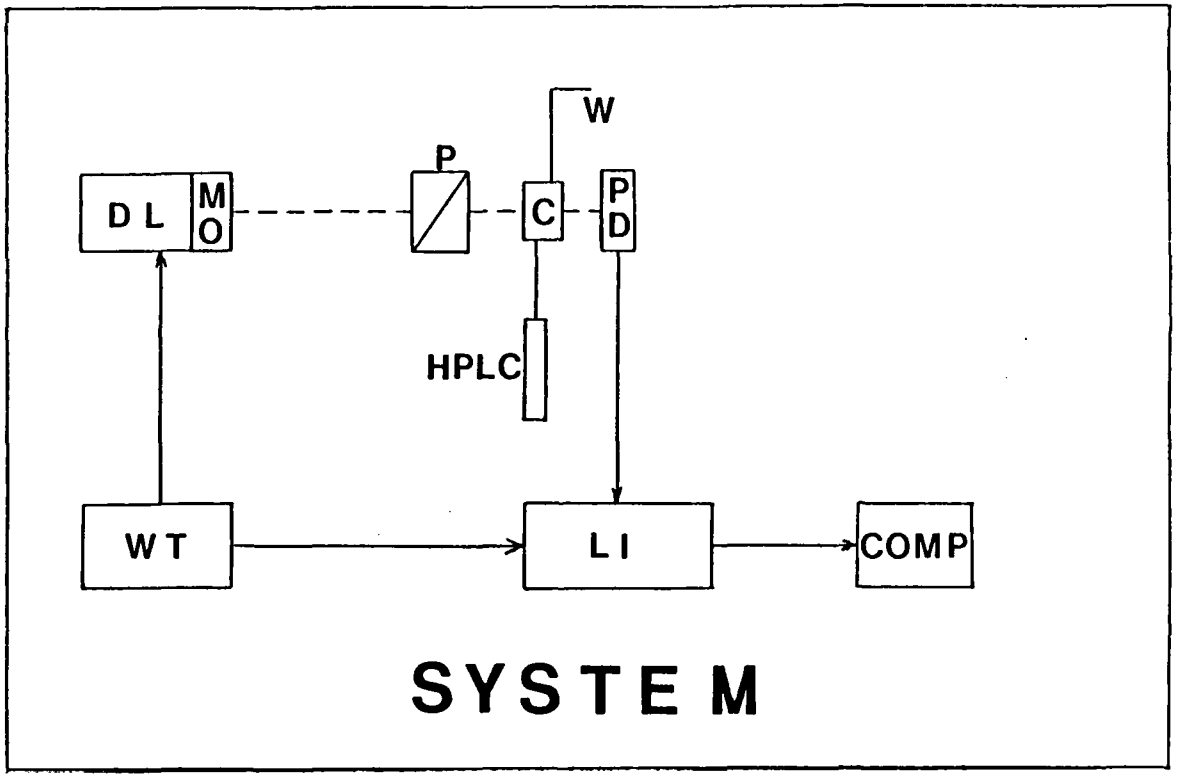

Figure 1. Schematic for RIG detection of HPLC effluents: DL, diode laser; MO, microscope objective; P, polarizer (not equired); C, flow cell (Figure 2); PD, photodiode detector; HPLC, summarized HPLC system; W waste; WT, waveform generator; LI, lock-in amplifier; COMP, computer or recording device.

Theory

When light is incident upon a RIG, the wavefront is refracted towards the region of higher RI (31). The exact nature, or shape, of the RIG is highly dependent upon hydrodynamic conditions (32), and necessarily requires an ordered flow pattern (33). The extent of the interaction between the flowing RIG and the incident light beam is highly angular dependent. For a z-configuration cell, as shown in Figure 2, near grazing angle incidence produces both reflection and transmission components of much complexity. From our studies, it was clear that working far enough away from grazing incidence may be accomplished by carefully tilting the z-configuration cell, while focusing an incident diode laser beam towards the bottom of the flow cell. Careful tilting of the flow cell, which acts as an etalon, is important for the interferometer function. The resultant experimental condition, shown in Figure 3, lends itself to explain the RIG signal measured "experimentally", which depends upon probe beam deflection, followed by the subsequent effect on the photodiode output as an active component in the single-mode diode laser interferometer.

To relate the observed deflection due to the RIG, dn/dx, to the subsequent transmitted beam intensity, one must begin with (34,35)

$$\frac{d}{ds}\left(n_o \frac{dr_o}{ds}\right) = \frac{dn}{dx} \qquad (1)$$

where dn/dx is colinear with a direction vector, r, as a

function of distance, x, and time, t. A unit vector r_o, in the direction of r, indicates the displacement of the probe beam from its original direction, while n_o is the uniform solvent RI, and S is a ray path relative to dn/dx. Furthermore, r_o and S are perpendicular to each other. Clearly, the maximum probe beam deflection occurs when dn/dx is perpendicular to S. This condition is exemplified in Figure 3, with $\phi = \pi/2$ radians, where ϕ is the angle formed between the incident beam direction and the direction of solvent flow. Note that in practice, ϕ is quite small, about 0.020 rad. Thus, eq 1 is more precisely written as

$$\frac{d}{dS}(n_o \frac{dr_o}{dS}) = \sin \phi \frac{dn}{dx} \qquad (2)$$

One wishes to measure the deflection angle, θ_d (t), for a given point of the RIG, dn/dx. Integrating both sides of eq 2 with respect to the ray path S yields

$$n_o \frac{dr_o}{dS} = \sin \phi \frac{dn}{dx} \int_o dS \qquad (3)$$

noting that the product sin ϕ dn/dx is essentially constant in the integration since the gradient moves at a rate much slower than the speed of light. The path integral $\int_o$ dS, in eq 3, is readily calculated since for small deflections

$$\int_o dS = L \qquad (4)$$

where L is the length of the RIG traversed by the probe beam, i.e., the flow cell length. Finally, the probe beam deflection of interest, θ_d (x,t) with respect to dn/dx, is readily available since for small deflections

$$\theta_d\ (x,t) = \frac{dr_o}{ds} \tag{5}$$

Combining eqs 3-5 and solving for $\theta_d\ (x,t)$ yields

$$\theta_d\ (x,t) = \frac{L}{n_o} \sin \phi\ \frac{dn}{dx} \tag{6}$$

which is consistent with previous work (26,27,35), except the angular dependence on ϕ has been included. The deflection angle $\theta_d\ (x,t)$ is related to solute concentration, C_x (volume fraction), by the chain rule since

$$\frac{dn}{dx} = \frac{dC}{dt} \cdot \frac{dt}{dx} \cdot \frac{dn}{dC} \tag{7}$$

Again, for low solute concentrations, typical in HPLC, the following approximation is made (15)

$$\frac{dn}{dC} = \frac{(n_o^2 + 2)^2}{6n_o} \left[\frac{n_x^2 - 1}{n_x^2 + 2} - \frac{n_o^2 - 1}{n_o^2 + 2}\right] \tag{8}$$

where n_o is the RI of a pure solute. Clearly, eq 8 is an indication of solute sensitivity in a given solvent. Substituting eq 7 into eq 6 yields

$$\theta_d\ (x,t) = \frac{L}{n_o} \sin \phi \cdot \frac{dC}{dt} \cdot \frac{dt}{dx} \cdot \frac{dn}{dC} \tag{9}$$

It is the change in $\theta_d\ (x,t)$ with time as a function of dC/dt, i.e., the concentration gradient, that ultimately leads to a change in the quantity of transmitted probe beam intensity measured by the photodiode. Note that dt/dx is

equal to 1/u, where u is the linear flow velocity. Experimentally, θ_d (x,t) may be measured by use of a position sensitive detector (PSD). The observed signal, α, at time t is given by

$$\alpha = K \cdot \theta_d (x,t) \cdot d \qquad (10)$$

where d is the distance from the probed gradient to the PSD and K is a proportionality constant converting distance to voltage.

Now, one needs to consider the measurement of θ_d (x,t), particularly in relation to dC/dt in eq 9. If a Gaussian peak shape is assumed, the concentration C (t) at time, t, of the analyte is given by

$$C(t) = \frac{C_i}{\sigma_t (2\pi)^{1/2}} \exp\left\{ -\tfrac{1}{2} \left(\frac{t_r - t}{\sigma_t} \right)^2 \right\} \qquad (11)$$

where $C_{x,i}$ is the injected analyte concentration, σ_t is the standard deviation of the analyte concentration profile at time, t, due to all broadening mechanisms, and t_R is the retention time of a given analyte (in the context of HPLC detection). Since the sensitivity depends upon θ_d (x,t), from eq 9, which depends upon C (t), the derivative of eq 11 with respect to t yields

$$\frac{dC}{dt} = C(t) \left[\frac{t_R - t}{\sigma_t^2} \right] \qquad (12)$$

Taking the derivative of dC/dt with respect to t and setting it equal to 0 allows one to calculate the maximum points of

sensitivity, which occur at $t = t_R \pm \sigma_t$ (26). Thus, the analytical signal measured by the RI gradient detector becomes the peak-to-peak signal, $\theta_d (x,t)_{p-p}$ (as in Figure 4), of the gradient response, at $t = t_R + \sigma_t$ and $t = t_R - \sigma_t$ for a Gaussian peak.

Substituting eq 12 into eq 9 yields

$$\theta_d (x,t) = C (t) \left(\frac{t_R - t}{\sigma_t^2}\right) \cdot \frac{1}{u} \cdot \frac{dn}{dC} \qquad (13)$$

Experimental measurement of $\theta_d (x,t)$ at $t = t_R \pm \sigma_t$ by use of eq 11 gives

$$C (t = t_R - \sigma_t) = \frac{V_i}{F} \quad \frac{C_i}{\sigma_t (2\pi)^{1/2}} \quad e^{-1/2} \qquad (14)$$

Of course $C(t = t_R + \sigma_t)$ gives the same result so that

$$\theta_d(x,t)_{p.p} = [\theta_d(x,t)(t = t_R - \sigma_t)] + [\theta_d(x,t)(t = t_R + \sigma_t)] \qquad (15)$$

and

$$\theta_d(x,t)_{p.p} = \frac{2V_i}{F} \quad \frac{C_i}{\sigma_t^2 (2\pi)^{1/2}} \quad e^{-1/2} \quad \frac{1}{u} \quad \frac{dn}{dC} \qquad (16)$$

Thus, measuring the signal with a position sensitive detector where the total angle of deflection is translated into a distance, α_{p-p}, we find from eq 10 and 16

$$\alpha_{p.p} = K \cdot \theta_d(x,t)_{p.p} \cdot d \qquad (17)$$

The volumetric flow rate is related to the cross-section area, A, by

$$F = uA \qquad (18)$$

where A equals πr^2, with r equal to the radius of the probed volume. Hence, eq 17, may be rewritten as

$$\alpha_{p\text{-}p} = K \cdot d \cdot \left(\frac{8\pi}{e}\right)^{1/2} \frac{r^3}{n_o} \frac{dn}{dC} \cdot \frac{V_i C_i}{\sigma_v^2} \qquad (19)$$

where the radius of expansion, r, equals (L sin ϕ)/2, and $\alpha_{p\text{-}p}$ is the experimentally measured peak-to-peak gradient signal. Besides the relatively easy PSD measurement of the RIG effect, one may simultaneously observe an interferometric signal via an intensity measurement. By carefully tuning the relative positions, both lateral and rotational, of the flow cell and photodiode, one achieves a signal from this interferometric mechanism that linearly correlates with eq 19 for over two orders of magnitude. The extreme stability of the laser diode light source plays an important role in observing this phenomenon. In this system, the noise (standard deviation) of the laser diode output was found to be 4 x 10^{-5} relative to the output intensity. It is interesting to note that the device is pathlength dependent. While eq 9 is a somewhat simplified version of what may be observed in this complex detection system, eq 19 contains more of the detail required to be analytically useful. Experimental simplicity and device applicability are readily obtainable and will be discussed in the context of universal HPLC detection.

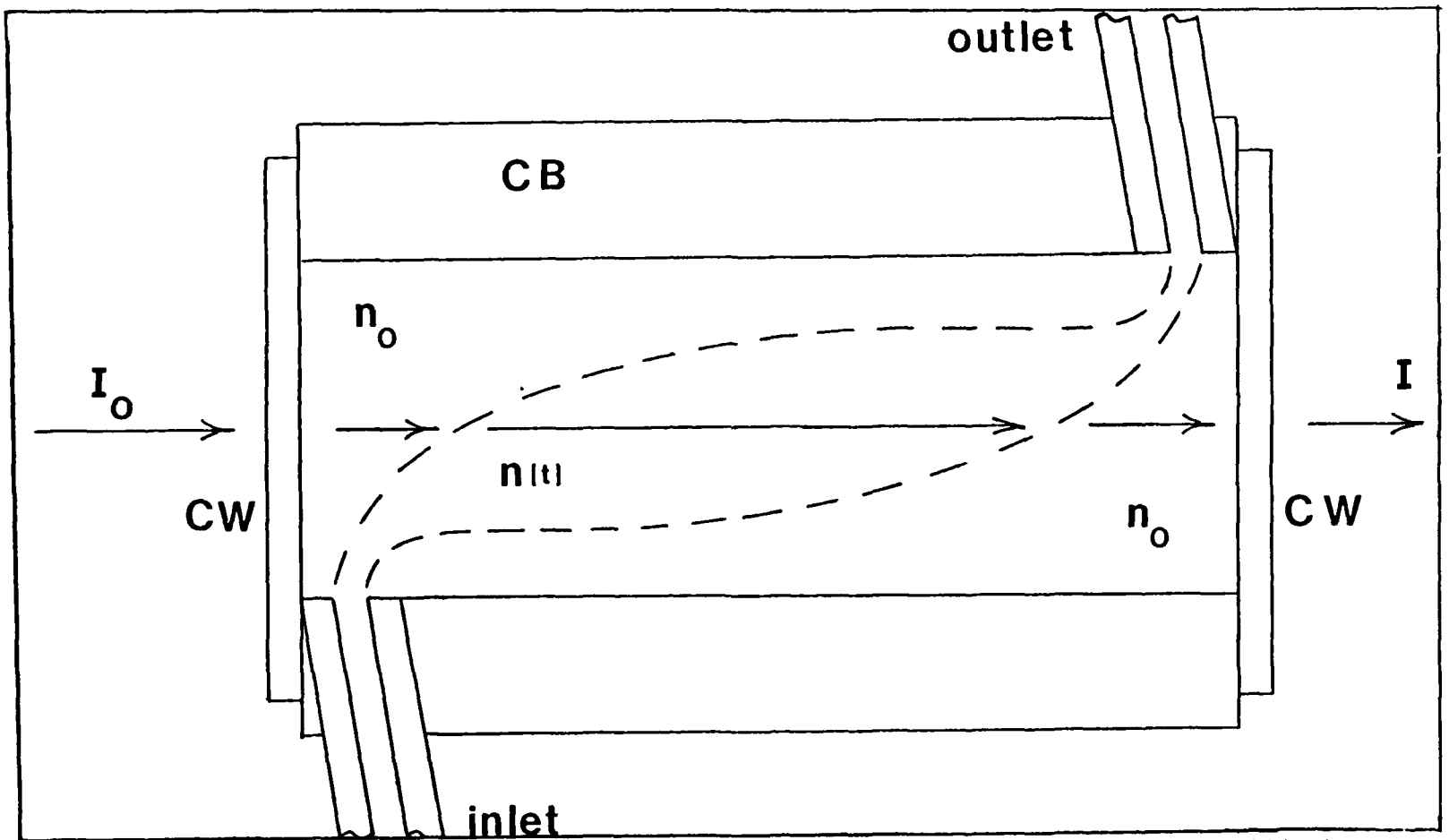

Figure 2. Flow cell Model: I_o, incident beam; I, transmitted beam; CW, cell window; CB, cell block (aluminum); n_o, eluent RI, n(t), time-dependent RI; inlet, from HPLC system; outlet, to waste.

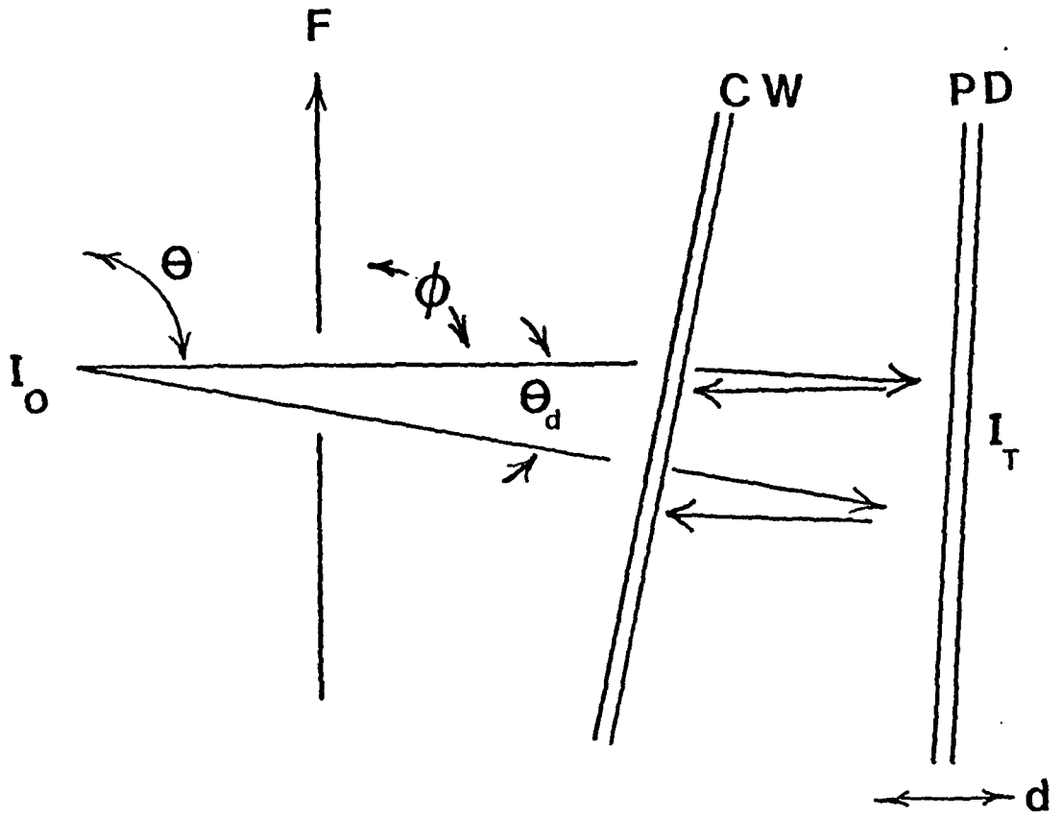

Figure 3. Detection of RI gradient model: I_o, incident beam; I_T, transmitted beam; F, direction of flow; CW, exit cell window; PD, photodiode; θ_d, detected angle due to RIG gradient presence; ϕ, incident angle to flow; θ, rotational tuning angle for flow cell; d, translational tuning distance for PD relative to CW.

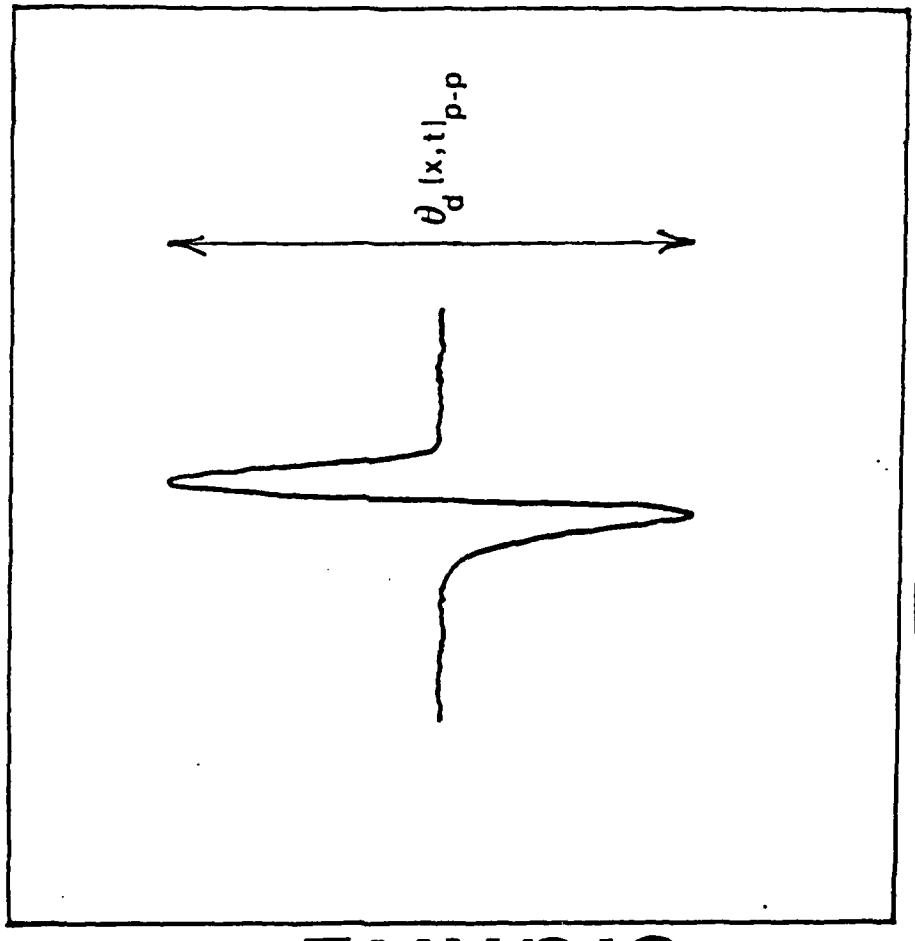

Figure 4. Typical signal.

Experimental

The primary experimental system is shown in Figure 1. Key variations of this design are seen in Figure 5 while minor changes are described below. In general, a 780 nm diode laser (Physitec Corp., DL 25, Norfolk, MA) with 3 mW output was intensity modulated at 20 kHz via a TTL waveform (Wavetek, Model 190, San Diego, CA) which was synchronized to a lock-in amplifier (Princeton Applied Research Corp., Model 5204, Princeton, NJ). A microscope objective, f16.85, designed for the diode laser system, focused the laser probe beam to a spot size of ca 200 um at a z-configuration cell (made in-house) at a focal length of ca 60 cm. Probe beam polarization was purified before entering the cell by passing the beam through a polarizer (Karl Lambrecht, MGTYS8, Chicago, IL) which was mounted in and precision tuned by a rotational stage (Newport, Model 471-A, Fountain Valley, Ca). A similar polarizer (functioning as an analyzer) and stage were placed between the cell and the detector as in Figure 5 for much of the early work. Two flow cells were constructed from aluminum and configured as in Figure 2. Each had a cylindrical bore 1.0 cm length by 800 um I.D. yielding a volume of 5.0 uL. The cell windows were glass microscope slide cover-slips (VWR Scientific Inc., 25 x 25 mm, #1 1/2, San Francisco, CA) carefully glued at each end of the cell. Entrance and exit tubing to the flow cell was Teflon, 1/16 inch O.D. x 0.007 inch I.D. nominal. After passing through the cell, the probe beam was

imaged onto a photodiode (Hamamatsu, S1723-05, Hamamatsu City, Japan) with a 1 cm x 1 cm active surface. The photodiode voltage output was sent to the lock-in amplifier to obtain the in-phase and subsequently demodulated analytical signal, synchronized by the waveform generator. The analytical signal was sent to either a personal computer (IBM-XT, Armonk, NY) via an interface board (Metrabyte, DASH-16, Taunton, MA), or a chart recorder (Houston Instruments, D-5000, Austin, TX) or simultaneously to both devices.

The flow cell was mounted on a high-precision translational stage (Newport, 460-XYZ, Fountain Valley, CA), while the detector was mounted on a similar stage for the translation studies and a high-precision rotational stage (Newport, Model 471-A, Fountain Valley, CA) otherwise. The fiber optic variant of Figure 5 consisted of a single-mode silica fiber positioned via a tilt stage (Newport, F-19TS, Fountain Valley, Ca) and fiber coupler (Newport, F-916T, Fountain Valley, CA). A 5X microscope objective after the analyzer focused the analytical beam into the fiber. The fiber was rigidly mounted through the case of and incident upon a pin photodiode (Hamamatsu, S1406-05, Hamamatsu City, Japan). The signal was then demodulated and recorded as previously described.

State-of-the-art HPLC systems (both standard and microbore) were used to introduce separated analytes into

the flow cell as well as simple injection of a sample plug into the flowing eluent stream. The complete HPLC work is described elsewhere (36). In all cases, injection was made through an injection valve (Rheodyne, Model 7125, Cotati, CA) into the eluent stream pumped by a high precision and high pressure syringe pump (ISCO, LC-2600, Lincoln, NE). Studies were made with water as the solvent for sugar samples (sucrose, fructose, glucose, and galactose) as well as polyethylene glycol samples (Polymer Laboratories, Amherst, MA), and with spectrograde CH_2Cl_2 as solvent with polystyrenes (Polymer Laboratories) as samples. Additional studies were conducted with toluene and dibutyl phthalate with 50/50 v/v acetonitrile and water as solvent. Columns used were a 250 x 4.6 mm I.D. Macrosphere, 300 A pore, 5 um, C8 standard column (Alltech, Deerfield, IL) and a 250 x 1.0 mm I.D., 300 A pore, 5 um, C8 microbore column (Brownlee Labs, RP300, Santa Clara, CA). The studies with toluene and dibutyl phthalate were done with a 60 x 2 mm I.D., 300 A pore, 5 um, C8 column (Alltech, Deerfield, IL).

Samples entered the flow cell after passing through either an HPLC column or a small length of Teflon tubing (0.007 inch I.D.) hereafter called "flow unit". Various lengths of tubing were used in the flow unit studies, with 85 cm generally used. The z-configuration flow cell yielded ordered flow from inlet to outlet at flowrates of 20 uL/min to 300 uL/min. Faster flowrates were evidently turbulent or

in transition to turbulence, causing a homogenous RI in the cell with resultant loss of useful analytical signal.

Initial experiments were conducted to determine the optimum flowrate for maximum sensitivity and to find the flowrate range where a useable analytical signal could be obtained. Subsequent studies were conducted at the flowrate yielding maximum sensitivity. For aqueous HPLC ca 60 uL/min was optimal while for HPLC with CH_2Cl_2 as eluent ca 40 uL/min proved best. The flow unit studies with CH_2Cl_2 as solvent were generally conducted at 107 uL/min.

With fixed flow cell conditions, the distance between the cell rear window and the photodiode was adjusted along the probe beam axis in 100 um increments, noting the detector response for injection of the same model solute at each step. Sensitivity varied significantly with detector position, but signal response did not decrease smoothly as in an inverse-square fashion, but in fact varied periodically as will be discussed. Further studies were then conducted with the detector fixed at the position yielding maximum response.

The flow cell was then rotated near normal incidence and detector response to the injected model solute noted at each angle. The angles at which maximum signal response occurred were noted. One might expect similar results from the corollary experiment, that of rotating the detector from normal incidence. This experiment was also conducted, but

otherwise the detector surface was fixed at normal incidence. The flow cell was also adjusted vertically (z-axis) and transversely (y-axis) with regard to the probe beam axis (x-axis). Translation in the z-axis significantly altered the signal response (as one would expect from the rotation study) while movement in the y-axis had essentially no effect (until striking the cell walls with the beam at the extremes). It was found that optimum tuning could be most readily obtained by cell rotation after centering the probe beam through cell midpoint. Rapid tuning was obtained by using a short (ca 25 cm) section of Teflon tubing (0.007 inch I.D.) in place of the HPLC columns.

Studies were also conducted to see if polarization effects were significant. Polarization crystals were used in several configurations: 1- ca. one cm before and after the flow cell, i.e., a polarizer/analyzer (P/A) combination, 2- polarizer only ca. one cm before the cell, 3- neither crystal in the optical train.

In several of the studies, comparison of signal detector response was made with a commercial UV-Vis absorbance detector for HPLC (ISCO, Model V4, Lincoln, NE) fitted with a 0.50 uL flowcell (ISCO, Series 0080-072, Lincoln, NE) having a pathlength of 2 mm. Additional studies were made with a position sensitive detector (PSD)(Hamamatsu, S1352, Hamamatsu City, Japan) of 2.5 x 33 mm dimensions. The PSD was placed 5 cm behind the exit

window of the flow cell and aligned such that vertical deflections of the laser beam would be detected. A comparison study with the PSD aligned horizontally was conducted, confirming, as suspected, that the primary beam deflection caused by solutes passing through the cell occurs in the vertical axis. The PSD was mounted on a high precision translational stage (Newport, 460-XYZ, Fountain Valley, CA) which not only allowed for precise positioning of the PSD, but accurate correlation of beam deflection with signal response. That is, the PSD was translated exactly 1 mm in the z-axis and the corresponding change in signal voltage measured. Then by simple geometry the deflection angle associated with a given analyte could be calculated (37). Prior to use of the PSD in recording analytical signals, the PSD was positioned to an electronic null and the ratio signal sent to the chart recorder. Subsequent analytical beam deflection signals appeared as deviations from this null baseline.

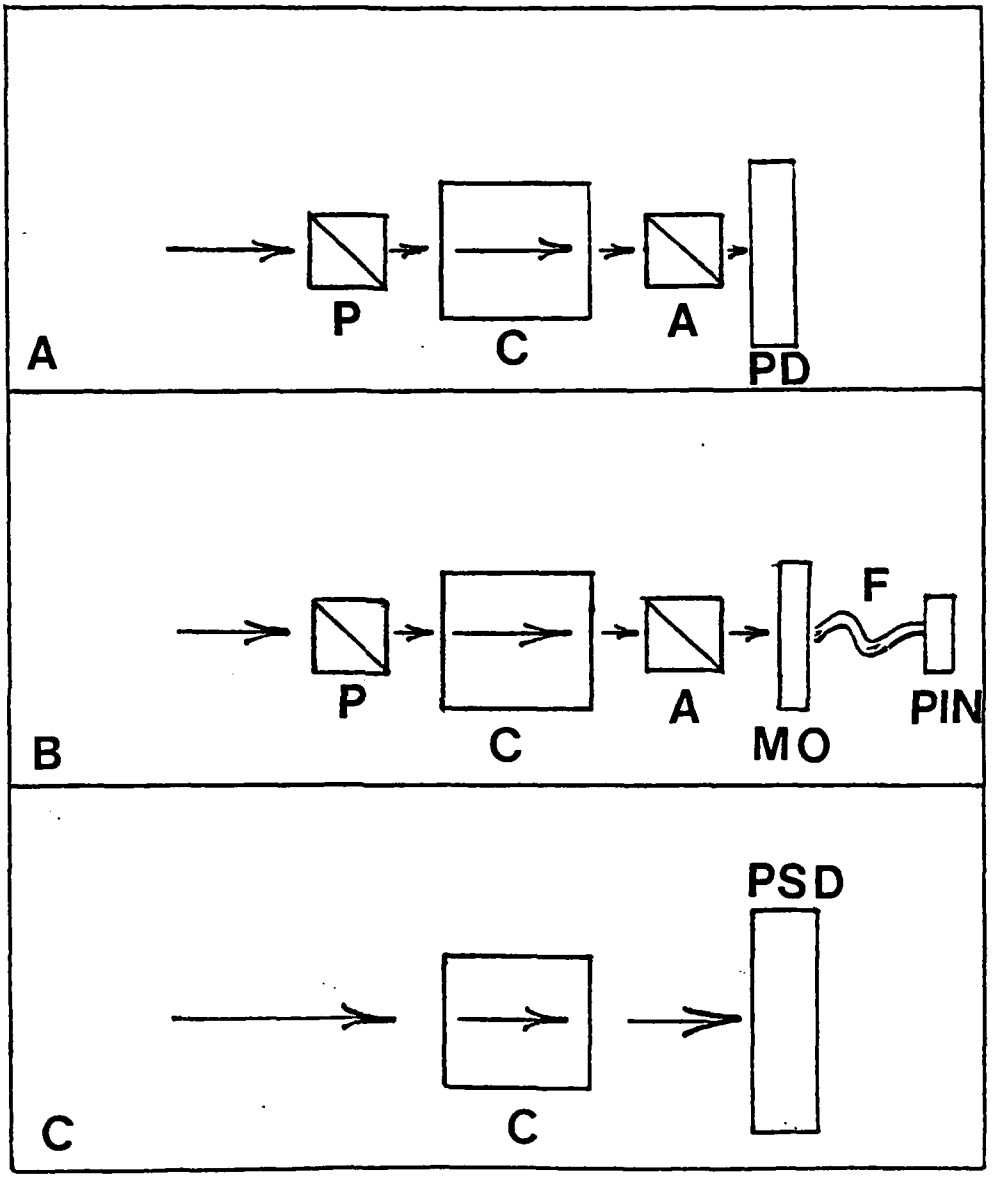

Figure 5. Variation Schematics; A - Polarizer/Analyzer version; B - Fiber Optic version; C - PSD version; Symbols: P, polarizer; C, cell; A, analyzer; PD, photodiode; MO, microscope objective; F, optical fiber; PIN, PIN photodiode; PSD, position sensitive detector..

Results and Discussion

The flowrate studies illustrate that signals may be obtained only in a specific range and that a rate for maximum sensitivity may be determined for a given solvent. For example, injection of a constant quantity of polyethylene glycol in water as the solvent caused a small chemical perturbation in the flow cell. The volumetric flowrate of the solvent was varied, thereby introducing change in the fluid motion in the cell. Measurement of the transmitted probe beam $I_T(t)$ due to the small but constant chemical perturbation according to eq 9 allowed changes in the hydrodynamic flow as a function of flow rate to be monitored. The results of this study are seen in Figure 6. Above ca. 300 uL/min, for this sytem, it is probable that turbulence prevails, yielding a homogeneous RI due to mixing throughout the flow cell. Hence no signal is obtained, for the physical condition of separate regions of stagnant and laminar flow as theorized no longer exist. Between 20 to 300 uL/min, however, a detector response was measured indicating $I_T(t)$ changed as a function of the chemical perturbation that was introduced.

This is strong evidence for the existence of "ordered" flow in the flow cell such that the condition modeled in Figure 2 may be a reasonable explanation of the observed results. Below 20 uL/min, the signal also falls off, and it appears that the volumetric flow rate was too slow to overcome serious diffusion effects in the flow cell or a

continual "sweeping out" of the flow cell corners occurs, thus destroying the different refractive index region boundaries as depicted in Figure 2. Although a priori Reynolds number calculations for the system are difficult due to the complicated experimental geometry, one would expect the Reynolds number calculations to yield the low values associated with laminar flow (i.e., less than 2000). Indeed, the extremely low values of Hagen - Pouisselle flow (less than 300 units) are obtained as summarized in Table 1. The values of Table 1 for the three solvent systems studied were calculated using the standard equation for fluid in a pipe

$$Re = \frac{dpv}{n} \qquad (20)$$

where Re is the Reynolds number for the solvent, d is the distance of the pipe (in this case, the flow cell length), p is the fluid density, v is the linear flow velocity, and n is the fluid viscosity.

Precise rotation of the flow cell, i.e., adusting θ in Figure 3, with subsequent detection of $I_T(t)$ for a constant concentration perturbation was conducted to examine the mechanism behind the detected intensity changes. Although initial computer simulation studies based on planar reflection losses yielded maxima and minima with spacing consistent with the experimental data, the magnitude of the intensity change observed could only be accounted for if an interferometric mechanism were operating. First, the

photodiode lateral position, d, was kept constant, and the flow cell rotated by 1.1 mrad increments (θ), spanning 100 mrad, with the center of the range approximately where the probe beam was perpendicular to the cell windows. At each incremental setting the photodiode output was measured. The photodiode output data are essentially the baseline signals, B(θ). An average baseline signal was calculated, B, and the relative difference calculated, B_{rel} (θ), at each incremental setting

$$B_{rel}(\theta) = \frac{B(\theta) - \bar{B}}{\bar{B}} \qquad (21)$$

with the results for a portion of the θ range traversed shown in Figure 7. The shape of B_{rel} (θ) versus θ increment in Figure 7 is consistent with an Airy function, with a depth of modulation of about 10% and a periodicity of 35 mrad (38). By injecting a suitable model solute at constant injected mass, flowrate (107 uL/min) and entrance tubing (28 cm of 0.007" I.D. Teflon), and detecting the RIG signal at each incremental angle, as for Figure 7, the relationship between B_{rel} (θ) and the RIG signal was studied. As previously reported (26,27), the RIG signal, θ_d in Figure 3, was measured as the peak-to-peak response, labeled as ∇C instead of θ_d $(x,t)_{p-p}$ or α_{p-p} since a gradient of concentration is effectively measured as the maximum to minimum deflection angle, given by eq 16 and 19. For a binary mixture with the solute at low volume fraction (15)

equation 8 may be used to calculate dn/dC. ∇C was measured at each incremental angle, θ, thus $\nabla C(\theta)$ is compared to $B_{rel}(\theta)$. These results are presented in Figure 8, where $\nabla C(\theta)$ and $(B(\theta)-\overline{B})/10$ are both plotted for approximately one full period in the Airy function (38). Referring back to eq 21, the quantity $(B(\theta)-\overline{B})/10$ is plotted instead of $B_{rel}(\theta)$ in order to simplify the plotting of Figure 8. Note that the $\nabla C(\theta)$ signal (peak-to-peak) is a positive value if the model solute RI is greater than solvent RI, as was the case for polystyrenes in CH_2Cl_2. It is clear from Figures 7 and 8 that there is a direct correlation between $B_{rel}(\theta)$ and $\nabla C(\theta)$, with the conclusion that flow cell rotational position, acting as an etalon, must be considered in the performance of the RIG interferometric detector. Clearly, with the flow cell at a fixed position, rotation of the detector surface instead of the flow cell should yield similar maxima and minima if an interferometric mechanism is operating, and such was indeed found to be true. Further confirmation that simple planar reflection losses are not the basis of the observed signal is the fact that rotation of the detector surface such that the incident light does not reflect back to the flow cell window results in total loss of signal associated with the chemical perturbation while measured background intensity remained constant. With detector geometry at near normal incidence to the light exiting the flow cell, the complex interferometric pattern

provides sensitive detection of intensity changes caused by chemical perturbation of the optical conditions in the flow cell.

One would expect then, to be able to find an optimal position at which the detector should be placed in order to most advantageously use this effect. The results of incrementally adjusting the detector along the probe beam axis are shown in Figure 9. Steps of 25 to 500 um were taken, with the baseline signal as a function of distance B(d) measured, analagous to B(θ) for flow cell rotation. Simultaneously, $\nabla C(d)$ was measured at each incremental distance for the same model solute as in $\nabla C(\theta)$ measurements. The results are shown in Figure 9, where $\nabla C(d)$ is plotted as a function of the lateral translational distance, d, in mm. B(d) has not been plotted in Figure 9 for clarity, although B(d) was correlated to $\nabla C(d)$ in the same way B(θ) was correlated to $\nabla C(\theta)$ in Figure 8. Clearly, translational positioning of the photodiode relative to the flow cell (Figure 9) produces an Airy function (38) analogous to Figures 7 and 8, where flow cell rotation was examined. It is interesting to note in Figure 9 that RIG detection sensitivity is optimized at 3.5 mm and 13.5 mm where large jumps in sensitivity were observed. The periodicity of the large jumps is about 20 mm. Underlying these large jumps in sensitivity is a $\nabla C(d)$ versus distance (d) dependence that is less pronounced. The periodicity of the less pronounced

sensitivity positions is about 8 mm. One would desire to work at an optimum in sensitivity, which occurs at either 3.5 or 13.5 mm lateral displacement between the flow cell exit window and the photodiode. In practice, satisfactory RIG detection sensitivity is obtained even if one works some distance from the optimum, but prior knowledge of the periodicity of a given RIG interferometric detector, for both flow cell rotation and photodiode lateral displacement, is essential for rapid day-to-day tuning. Each data point in Figure 9 corresponds to the same chemical perturbation. Reversal of the pattern evidently occurs at ca 8.5 mm; the signal is then negative with respect to baseline but of similar magnitude. Although we do not give a mathematical description of the interferometric pattern observed, one can appreciate the temporal and spatial aspects involved with the interference zone by referring to the work of Brayton (39), Siegman (40), and the discussion in (41). Nevertheless, the application of the optical effect is straightforward, i.e., adjustment of the cell rotation angle and translation of the detector to obtain maximum signal response for the same chemical perturbation in the flow cell.

In the effort to understand the observed effect, studies were done with polarizers in the optical train as previously described. No significant polarization effects were observed, and indeed, the device works quite

satisfactorily without the use of polarizers or any other optical filters. The fiber optic variant Figure 5 performed satisfactorily as well and the depicted configuration could be used to observe the phenomenon if desired.

An additional question to address in connection with this device is that of optical feedback. Dandridge (28-30) successfully employed optical feedback into a diode laser to achieve distance resolutions of 9 x 10^{-5} nm. Is the observed signal produced or largely influenced by an optical feedback mechanism to the diode laser cavity instead of or in concert with the proposed interferometry? Such was found not to be the case. Deliberate feedback of the beam into the laser cavity using the described geometry did not produce any measurable intensity changes.

It is important to note that the characteristic properties of the diode laser (1,42) are critical to the observance of this phenomemon. In particular, the low noise (standard deviation of 4 x 10^{-5} relative to output intensity) of the laser and the extremely long coherence length (at least 10 m) give the stability required to observe the signal above background, a signal which would be swamped by the greater noise and instability associated with other typical laboratory lasers such as a He-Ne laser.

The deflection of the laser probe beam resulting from the refractive index gradient as a solute transits the flow cell may be followed either by the intensity changes

associated with the interferometric mechanism incident on a photodiode surface or by use of a position sensitive detector. Both methods were studied and each has advantages which may be exploited as discussed in turn below.

Although more complex and difficult to describe mathematically, the interferometric method is extremely sensitive, yielding a mass limit of detection (LOD) of 540 pg injected for 500,000 g/mole polystyrene, or 1.1×10^{-15} moles when coupled with microbore HPLC. Alternatively, the injected concentration for the 500,000 g/mole polystyrene at the LOD was 0.9 ppm or 2.4 nM. Inferred refractive index changes of 4×10^{-9} RI can be measured, had the concentration level at the LOD been measured by conventional RI detection approaches (3). The linear dynamic range extends from the limit of detection through two orders of magnitude. At higher concentrations, deflection moves through orders of fringes in the interferometric pattern, making it difficult to deconvolute the resultant signal. The PSD would be appropriate, then, when extremely sensitive measurement is not required. Nevertheless, the interferometric system may be tuned fairly rapidly and need not be precisely adjusted unless maximum sensitivity is desired.

Use of the linear PSD in lieu of the photodiode is advantageous in the sense that the deflection angle can be readily measured and mathematically ascribed. It is simpler

to set up and does not require the same precision of tuning as the interferometric method. The only adjustment required beyond basic beam centering is translation of the detector along its major axis to find the signal null which allows use of the device without extinguishing room lights. The signals obtained with the PSD were consistently smooth derivative shaped curves which were easily treated mathematically and could easily be integrated, if desired, to obtain a more conventional shape, and perhaps improve detectability simultaneously via the integration (35,43). The same PSD was employed by Renn and Synovec (37) who obtained ca 1 um resolution. Since that study, an electronic component was replaced to increase the resolution to optimum, measured to be Ø.6 um (3σ) in connection with these studies.

A significant advantage of the PSD is detection of the direction of the beam deflection, leading to better understanding of the flow cell deflection mechanism. With the PSD it is possible to clearly compare results obtained experimentally with the expected signal given by eq 19, which is the currently accepted theoretical relation. The device gives analytical signals that are orders of magnitude larger than expected. The unique flow dynamics associated with this device are apparently responsible for this extraordinary increase in sensitivity, and further study should result in the mathematical expression that more

completely describes the expected signal instead of eq 19.

It is, of course, necessary to position the PSD such that its axis is aligned with the axis of beam deflection to achieve maximum sensitivity. Comparison of the PSD aligned in the vertical axis (found to be the primary axis of beam deflection) yielded 4 times the sensitivity versus alignment in the horizontal axis (probe beam axis held constant).

Of particular interest is the possible use of this device as a detector for gradient HPLC. Of course, standard refractive index detectors cannot be used in gradient chromatography, for the response due to the changing refractive index of the gradient solvent overwhelms any slight RI change due to an analyte. This is a severe limitation associated with a standard RI detector.

Measurement of the refractive index gradient eliminates this limitation. To illustrate the viability of using this device for gradient HPLC detection, a large 100 uL injection loop was employed such that, for whatever material was injected, the central portion of the injected sample plug would remain essentially constant through the time required to flow through the flow cell. A 120 cm length of 0.007" I.D. Teflon tubing (30 uL volume) was used to introduce samples to the flow cell in place of an HPLC column. The refractive index gradient detector should return to baseline during the central position of the sample plug since dC/dt (and of course, dn/dt) is zero. By injecting samples of

pure compounds with widely different refractive index values, the relative shift in baseline could be measured and the viability of use of the device for gradient HPLC ascertained. As seen in Figure 10 there is no competition between RI response of the solvent and the gradient signal associated with an analyte. That is, since the refractive index gradient detector responds only to acute changes in RI, the RIG signal does not deviate substantially from the baseline condition either when the effuent RI is constant or linearly changing with time, even if the effluent RI is different than the original baseline solvent composition. Examined mathematically, one starts with eq 9 which predicts the probe beam angle $\theta_d(x,t)$ as a function of the material passing through the flow cell. A gradient may be produced by changing from C_A to C_B for solvents A and B (volume fractions). If the solvent gradient linearly changes from C_A to C_B with time, eq 9 suggests that the gradient of C_d (t) produces a baseline signal that is finite, yet constant, with time.

$$\nabla C_d(t) = C_B - C_A \qquad (22)$$

That one may assume the RI change as a function of eluent composition is nearly linear was exemplified by Woodruff and Yeung using a volume delay between sample and reference cells to produce a workable RIG (25). As seen in Figure 10, the baseline deviation shifts only ca 10 mV for 1 full unit change in refractive index. This corresponds to ca 6×10^{-2}

nV when operating near the limit of detection where the noise (5σ) is typically on the order of 10nV (using the interferometric method). Clearly, then, the gradual RI change of the solvent gradient is negligible in regard to the refractive gradient signal that is measured by the device.

Injection of a polystyrene standard with the same flow unit and large injection loop just described, followed by UV-Vis detection at 260 nm produced the signal shown in Figure 11. Note that a plateau region is present for an extended period of time, in which the solute concentration is finite, yet constant, with time. Analogously, in this plateau region the mixture RI is constant, yet different, from the baseline RI (solvent only). If the RI gradient detector is indeed also measuring the solute concentration gradient, then numerical differentiation of Figure 11 should produce the solute concentration gradient profile to be measured with the new RI gradient detector. The finite differential of the UV-Vis solute profile of Figure 11 is shown in Figure 12. In comparison, the RI gradient sensor produced, for three consecutive injections, the signals shown in Figure 13. Note the marked similarity between the differential of the UV-Vis absorbance detector data, Figure 12, and the RI gradient detector data, Figure 13. The comparison between Figures 12 and 13 strongly supports the interpretation of the response obtained with the novel RI

gradient detector. Clearly, when properly aligned, the new detector provides a signal that is identical to a concentration gradient, consistent with the explained mechanism leading from eq 9.

Table I. Solvent System Reynolds Numbers

Solvent System	Density g/mL	Flowrate mL/min	Viscosity poise	Re
H_2O	0.9991	20-300	0.0114	6-90
CH_2Cl_2	1.2166[b]	20-300	0.0045	20-295
H_2O/CH_3CN	0.8920[b,c]	20-300	0.0069[c]	9-130

a) Values of 15° C used except as noted.
b) 20° C value.
c) Calculated by average.

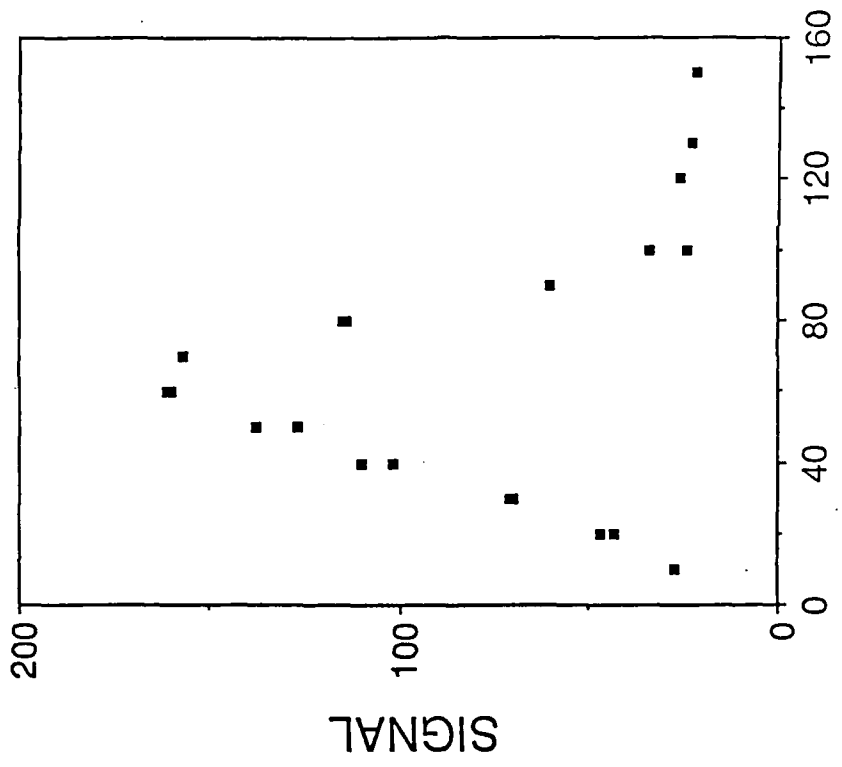

Figure 6. Flowrate study: Polyethylene glycol in water with flow unit

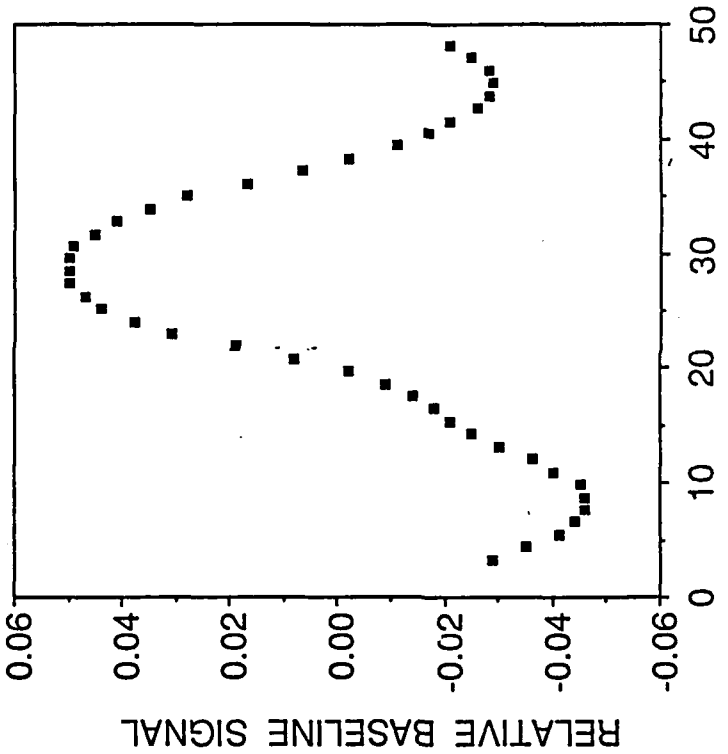

Figure 7. Relative baseline signal vs. flow cell rotation: calculated as (B(θ) - B)/10 as a function of angle increment, θ, for flow cell rotation with the interferometric RIG detector.

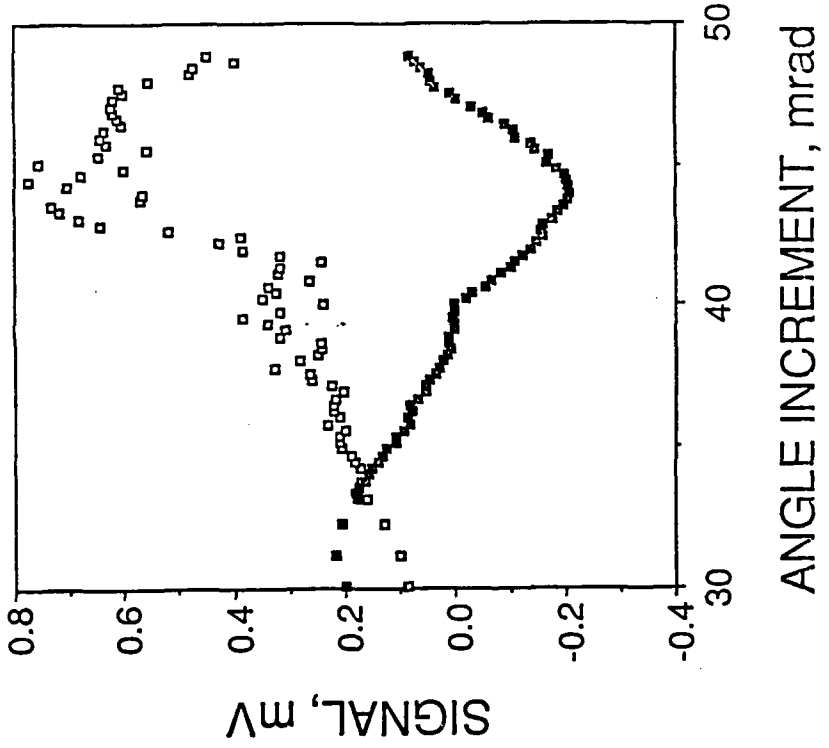

Figure 8. Relative baseline signal, $B_{rel}(\theta)$: ■ , and RIG signal, $\nabla C(\theta)$: □ , for flow cell rotation.

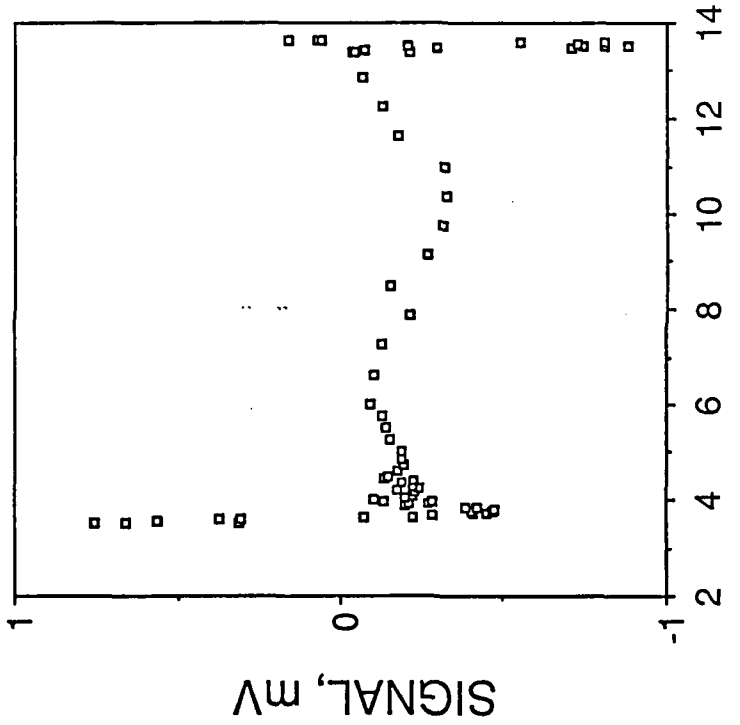

Figure 9. RIG signal ▽C(d):□, as a function of photodiode lateral displacement from the flow cell exit window with the interferometric RIG detector.

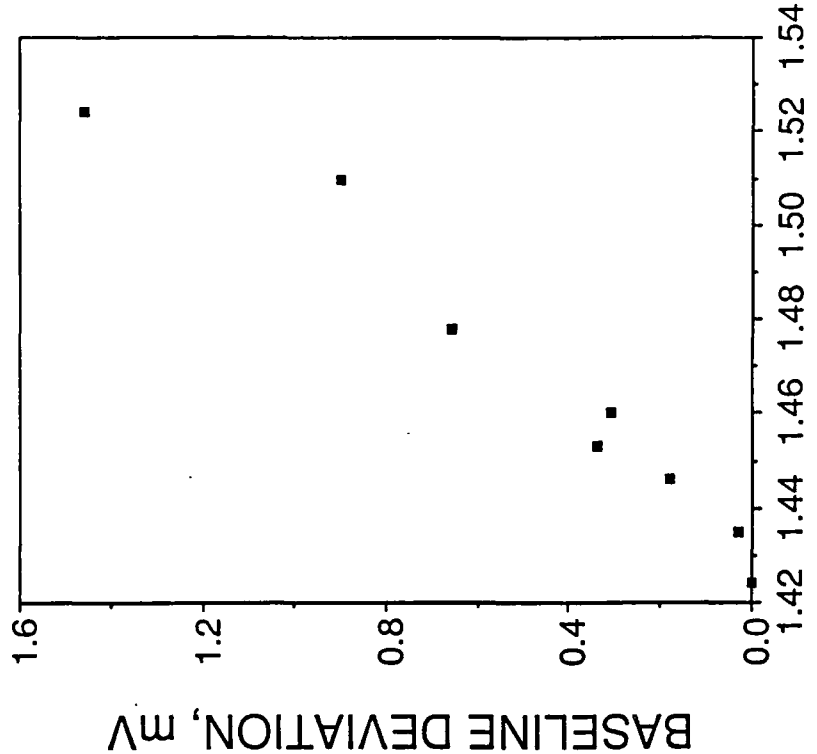

Figure 10. Relative baseline vs. RI for pure injected solvents

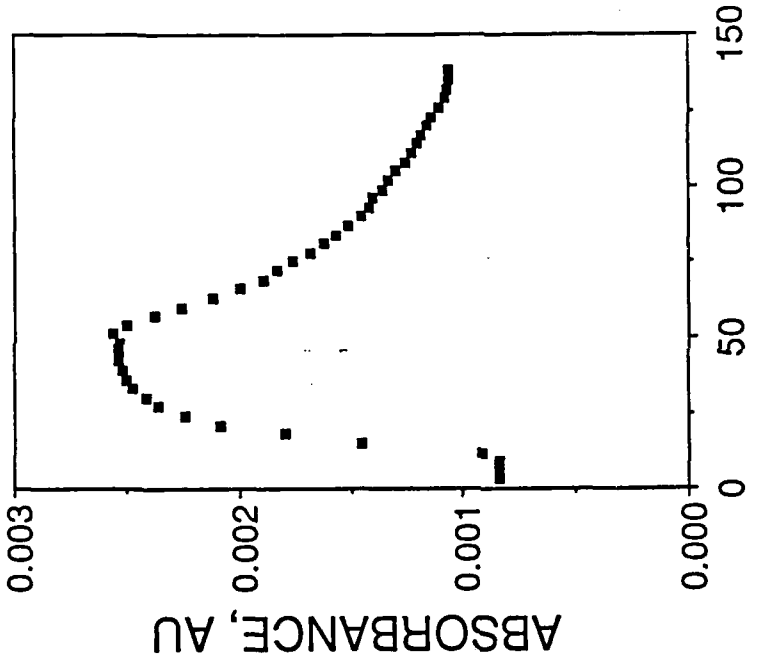

Figure 11. Absorbance signal as a function of time for a polystyrene standard injected such that a steady-state concentration is reached, and the signal reaches a plateau.

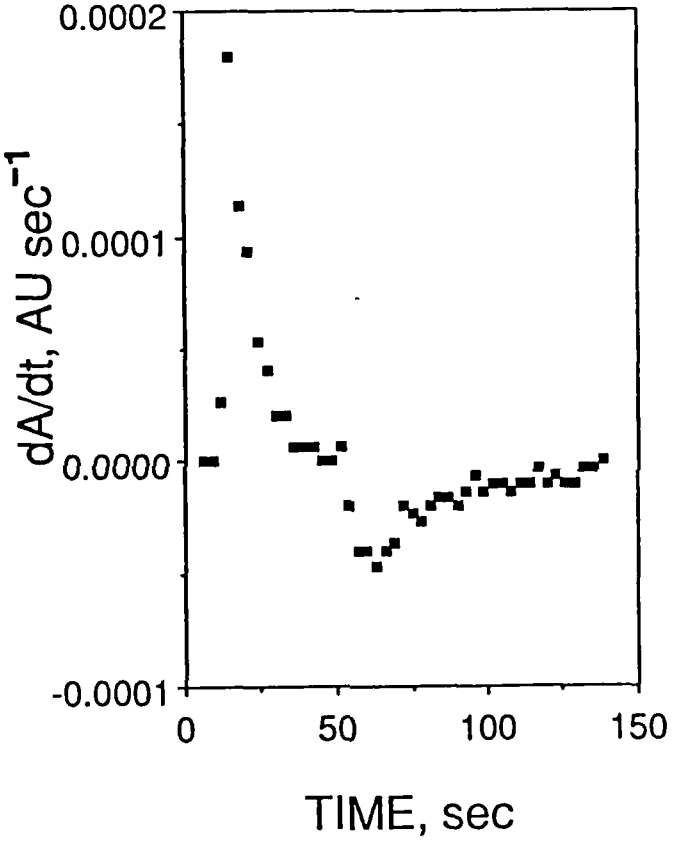

Figure 12. Time derivative of absorbance signal of Figure 11.

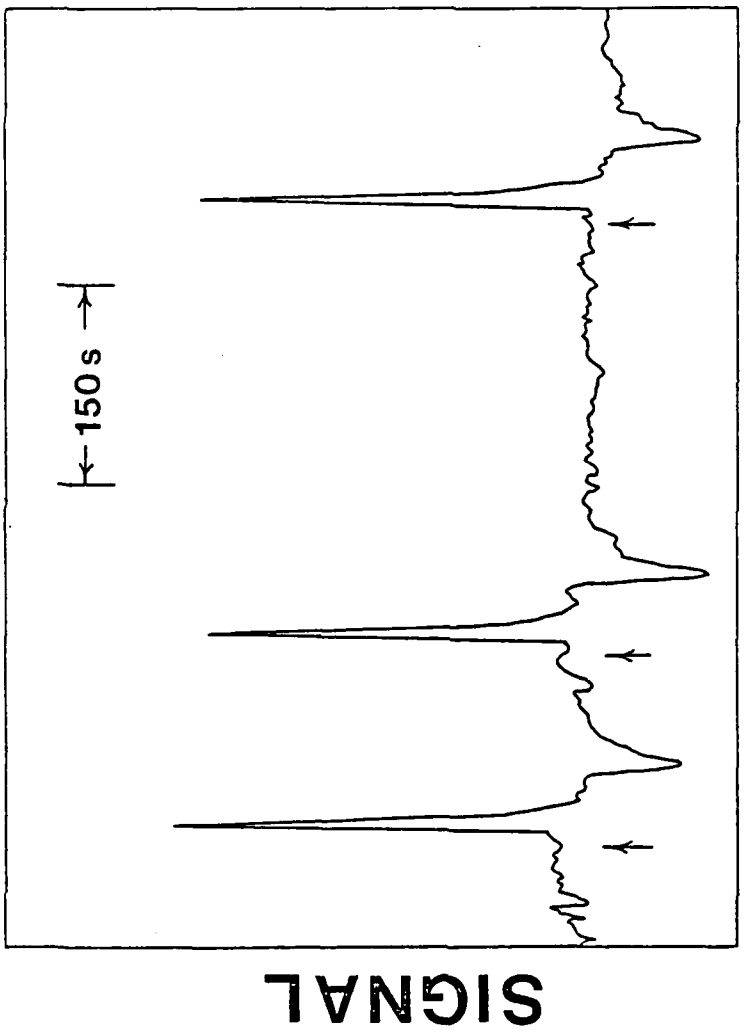

Figure 13. Three successive injections (noted by arrows) of the same sample and system as per Figure 11 followed by detection with the RIG detector. Note comparison to Figure 12.

Conclusion

The refractive index gradient detector, with further improvements, may well be the universal detector of choice for HPLC, with a present demonstrated detection limit of 4×10^{-9} RI units (rms). This detection limit was calculated for a known injected volume fraction of 500,000 g/mole polystyrene in CH_2Cl_2. However, as inferred by eq 19, any improvement in the separation efficiency, reducing σ_z^2, will result in an improved detection limit. This will require a concurrent decrease in the flow cell volume to limit band broadening at detection. The flow cell volume was just small enough to limit broadening in the microbore HPLC of polymers (36) since the flow cell volume was about a factor of 10 less than detected solute peak volumes.

Since the RI gradient signal is quite sensitive to the eluting solute peak width, according to eq 19, it should be possible to exploit this dependence to more sensitively probe changes in polymer samples, as may occur in processing conditions. In particular, the flow unit could be used to rapidly assess the polydispersity of a polymer sample or to characterize linear and branched polymers. Polymer molecular weight and polydispersity generally require continuous monitoring to achieve consistent products, and it would be extremely useful to measure the polymer molecular weight and polydispersity directly. Since the RIG detector sensitivity is highly dependent upon the variance of the solute elution profile (26,27), one could use the flow

method to take advantage of the hydrodynamic properties of dilute polymer solutions to sensitively distinguish polymers based upon translational diffusion differences, which influence the solute elution profile variance. To accomplish such a task, one would need to consider all contributions to solute broadening, or dispersion, since both flow and spontaneous translational diffusion are coupled (44-48). However, if one operated under experimental conditions such that the spontaneous broadening of the solute profile as it enters the flow cell (which is governed by hydrodynamic behavior) dominated over all other broadening mechanisms, then this broadening effect would be dependent upon the translational diffusion properties of the solute in the solvent. The net result would be to encode solute size properties into the detected solute concentration profile, which would be sensitively monitored by the RIG detector.

The ability to obtain molecular size information without chromatography or elaborate studies would indeed be extremely useful. Calibration curves could be established rapidly, with the flow method well suited to process control applications. As a tool for theoretical studies, the flow method should offer a viable alternative to either light scattering or ultracentrifugation for providing molecular size information, as correlated to translational diffusion properties of macromolecules. The capability of the device

for the study of very dilute solutions, 5 x 10^{-4} to about 1 x 10^{-6} g/ml, would allow one to assume "infinite" dilution conditions for many applications. In some cases, it may prove important to put another detector in series and down-line from the RIG detector to provide necessary normalization to constant injected solute mass, in order to construct the calibration of RIG data to molecular size properties. The RIG detector may also prove useful if interfaced with field flow fractionation (49-51).

As currently developed, the refractive index gradient detector has many useful characteristics which make it extremely attractive as the detector of choice in a variety of applications. It yields universal detection. Since a non-absorbing wavelength (780 nm) is used, there is no requirement to search for a transparent solvent as is the case with absorbance detectors. Also, since detection is not based on absorption, no derivatization is required to enhance detector sensitivity and no wavelength selection element (e.g., monochromator) is required. For that matter, wavelength interference, often a problem with absorbance based detectors, would be rare since few chemical species absorb at this wavelength. Comparison studies with a UV-Vis detector have shown that the RIG detector exceeds the UV-Vis LOD even at excellent absorbing wavelengths and, of course, is far superior in the many analytical cases when a good absorbing wavelength is unavailable. The system is very

simple to set up and operate, particularly when using the PSD version. In fact, in the majority of cases the PSD version would be the configuration of choice due to its extreme simplicity and ease of operation compared to the interferometric version.

The prospects of conducting rapid polymer characterization and process monitoring are especially promising. And unlike conventional RI detectors, the RIG detector may be used with gradients, as previously discussed.

The detector should be very amenable to incorporation into a small portable device. The integral components of the diode laser head, associated power supply, objective lens, flow cell, and photodiode could easily be built into a compact unit, with a chamber built-in for rapid interchange of various types of flow cells. Optimal positioning of the device could easily be accomplished with a rotational micrometer positioning thumbwheel for the angular orientation of the flow cell, and a similar translational micrometer for positioning the photodiode surface. For extremely sensitive detection in the interferometric mode, piezoeletric final positioning could be done, and a feedback circuit built-in to maintain fine positioning for optimal performance. Electrical connections to facilitate data acquisition would complete the unit.

LIST OF REFERENCES

1. O'Shea, D.C.; Callen, W.R.; Rhodes, W.T. "An Introduction to Lasers and Their Applications," Addison-Wesley: Reading, Mass., 1978, Chapters 2 and 6.

2. Ikeda, M.; Honda, M.; Mori, Y.; Kaneko, K.; Watanabe, N. Appl. Phys. Lett., 1984, 45, 964.

3. Yeung, E.S.; Synovec, R.E. Anal. Chem. 1986, 58, 1237A-1256A.

4. Yeung, E.S., in Elving, P.J. and Winefordner, J.D. Eds., Chemical Analysis, Detectors for Liquid Chromatography, Vol. 89, Wiley-Interscience, New York, 1986.

5. Munk, M.N., in Vickrey, T.M. Ed., Liquid Chromatography Detectors, Dekker, New York, 1983.

6. Scott, R.P.W., Liquid Chromatography Detectors, Elsevier, Amsterdam, 1977.

7. Stolyhwo, A.; Colin, H.; Guichon, G. J. Chromatogr. 1983, 265, 1-18.

8. Stolyhwo, A.; Colin, H.; Guichon, G. Anal. Chem. 1985, 57, 1342-1354.

9. Berry, V.V. J. Chromatogr. 1980, 199, 219-238.

10. Berry, V.V. J. Chromatogr. 1982, 236, 279-296.

11. VanDerWal, S.; Snyder, L.R. J.Chromatogr. 1983, 255, 463-474.

12. Small, H.; Miller, T.E. Anal. Chem. 1982, 54, 462-469.

13. Bobbitt, D.R.; Yeung, E.S. Anal. Chem. 1984, 56, 1577-1581.

14. Mho, S.I.; Yeung, E.S. Anal. Chem. 1985, 57, 2253-2256.

15. Synovec, R.E.; Yeung, E.S. Anal. Chem. 1983, 55, 1599-1603.

16. Synovec, R.E.; Yeung, E.S. J. Chromatogr. 1984, 283, 183-190,

17. Synovec, R.E.; Yeung, E.S. Anal. Chem. 1984, 56, 1452-1457.

18. Synovec, R.E.; Yeung, E.S. J. Chrom. Sci. 1984, 23, 214-221.

19. Bornhop, D.J.; Dovichi, N.J. Anal. Chem. 1986, 58, 504-505.

20. Bornhop, D.J.; Nolan, T.G.; Dovichi, N.J. J. Chromatogr. 1987, 384, 181-187.

21. Bornhop, D.J.; Dovichi, N.J. Anal. Chem. 1987, 59, 1632-1636.

22. Synovec, R.E. Anal. Chem. 1987, 59, 2877-2884.

23. Wilson, S.A.; Yeung, E.S. Anal. Chem. 1985, 57, 2611-2614.

24. Woodruff, S.D.; Yeung, E.S. Anal. Chem. 1982, 54, 2124-2125.

25. Woodruff, S.D.; Yeung, E.S. J. Chromatogr. 1983, 260, 363-369.

26. Pawliszyn, J. Anal. Chem. 1986, 58, 243-246.

27. Pawliszyn, J. Anal. Chem. 1986, 58, 3207-3215.

28. Dandridge, A.; Miles, R.O.; Giallorenzi, T.G. Electron Lett. 1980, 16, 948-949.

29. Dandridge, A. Appl. Opt. 1981, 20, 2336-2337.

30. Dandridge, A.; Tveten, A.B. Appl. Opt. 1981, 20, 2337-2339.

31. Born, M.; Wolf, E. Principles of Optics, 6th ed., 1980, Pergamon Press, Great Britain, pp.121-1240.

32. Kachel, V.; Menke, E., in Melamed, M.R.; Mullaney, P.F.; Mendelson, M.L., Eds., Flow Cytometry and Sorting, Hydrodynamic Properties of Flow Cytometric Instruments, Ch. 3, John Wiley and Sons, New York, 1979.

33. Lighthill, J. Waves in Fluids, Cambridge University Press, Cambridge, 1978, pp.286-298.

34. Born, M.; Wolf, E. Principles of Optics, 6th ed., 1980, Pergamon Press, Great Britain. pp.41-47.

35. Jackson, W.B.; Amer, N.M.; Baccara, A.C.; Fournier, D. Appl. Opt. 1981, 20, 1333-1344.

36. Hancock, D.O.; Synovec, R.E. Anal. Chem. 1988, (submitted).

37. Renn, C.N.; Synovec, R.E. Anal. Chem. 1988, 60, 200-204.

38. Hecht, E.; Zajac, A. Optics, Addison-Nesley: Reading, MA, 1979, Ch. 9, pp.301-307.

39. Brayton, D.B. Appl. Opt. 13, 1974, 2346.

40. Siegman, A.E. J. Opt. Soc. Am. 1977, 67, 545.

41. Eichler, H.J.; Gunter, P.; Pohl, D.W.: Laser Induced Dynamic Gratings, Springer-Verlag, Berlin, 1986.

42. Salathe, R.P. Applied Physics, 1979, 20, 1-18.

43. Synovec, R.E.; Yeung, E.S. Anal. Chem. 1986, 58, 2093-2095.

44. Golay, M.J.E.; Atwood, J.G. J. Chromatogr. 1979, 186, 353-370.

45. Atwood, J.G.; Golay, M.J.E. J. Chromatogr. 1981, 218, 97-122.

46. Hupe, K.-P.; Jonker, R.J.; Rozing, G. J. Chromatogr. 1984, 285, 253-265.

47. Gareil, P.; Rosset, R. J. Chromatogr. Sci. 1985, 20, 367-371.

48. Rocca, J.L.; Higgins, J.W.; Brownlee, R.G. J. Chromatogr. Sci. 1985, 23, 106-113.

49. Giddings, J.C. J. Chem. Phys. 1968, 49, 81-85.

50. Kirkland, J.J.; Yau, W.W. Science 1982, 218, 121-127.

51. Caldwell, K.D. in "Chemical Analysis: Modern Methods of Particle Size Analysis," Barth, H.G., Ed, Wiley: New York, Volume 73, 1984, Chapter 7.